Energy Absorption Characteristics of Metallic and Composite Shells

R. Velmurugan

Indian Institute of Technology Madras, Chennai–600 036

and

N.K. Gupta

Indian Institute of Technology Delhi, New Delhi–110 016

ABSTRACT

Metallic and composite shells of different sizes and tubes were subjected to axial compression in an Instron Machine. Their progressive failure modes and energy absorption capacities have been studied. In the case of metallic shells, analytical expressions are derived to find the mean collapse load and the fold length based on the formation of plastic hinges. Theoretical results have been compared with experimental results wherever possible. The effect of internal folding on the post-collapse behaviour of round tubes has been discussed and expressions for fold length and post-collapse load compression curves are derived as a function of internal folding. Based on the experimental observations, analysis has been carried out to find the progressive crushing load and crush length in a cycle of round and conical shells. The shells are infilled with polyurethane foam and subjected to axial compression. The effect of foam on the crushing behaviour is also studied. Conical shells of different cone angles (varied from 8.5° to 45° and the effect of cone angle on the crushing mode of the conical shells has been studied. Also, a comparative study of metallic and composite shells has been carried out based on the deformation and energy absorption characteristics. The different parameters considered for analysis include effective crushing length and total energy absorbed during the crushing process and the Euler buckling length in metallic shells.

Keywords: Axial compression, metallic tubes, composite shells, failure mode, energy absorption, post-collapse behaviour

NOMENCLATURE

$W_h, W_h, W_m,$ W_f, W_t	Energy terms	R, t	Radius and thickness of shell
		t_1, t_2	Thickness of plies bending inside and outside the shell radius
		ϕ	Cone angle
M_{o1}, M_{o2}	Perfectly plastic bending moment capacity of the laminate bending inside and outside the shell thickness	θ, β	Bending angles of the plies
		h	Crush length
σ_o	Ultimate stress in axial tension	σ_m	Matrix shear strength

μ	Coefficient of friction
D_b, D_s	Base and narrow-end diameter of the cone
H	Height of conical shell
δ	Vertical deformation
P	Applied load
k	Ratio of t_1 to t
D	Mean diameter of tubes
W_T	Total strain energy in a fold or crush cycle
W_P	Work done by the applied load in a single fold or crush cycle
L	Half-fold length in metal tubes and crush length
σ_θ	Hoop stress of the laminate
δ_1, δ_2	Horizontal displacements of the conical shells, respectively
δ, δ_x	Axial compression and axial deformation of laminate
P, P_m	Axial load and mean collapse load
P_o	Ultimate load in uniaxial tension
m	Folding parameter (ratio of internal fold to the fold length)
M_p, M_p'	Maximum and reduced bending moment capacity per unit length
L_{in}, L_{out}	Internal and external fold lengths
N	Ratio of internal fold to external fold
D_{in}, D_o	Inner and outer diameters of tube.

1. INTRODUCTION

Thin-walled metallic and composite shells are widely used in aerospace and other automotive industries as energy absorbing elements. These elements deform into various failure and crushing modes when subjected to axial compression. The failure mechanism of such shells have been efficiently utilised in the design for crashworthiness.

Several experimental and theoretical studies have been carried out in the past[1-15]. Johnson and Mamalis[1] suggested various energy dissipating systems in cars, trains, and aircraft, which include: (i) the bumpers made of honeycomb plastics in cars, (ii) buffers with the destructible elements in trains, and (iii) plastically-deformable fuselage belly in aircraft. The deformation mechanism of various structural elements have been studied by Wierzbicki and Jones[2,3] and Gupta[4].

The axisymmetric folding of round metallic tubes has been investigated by many researchers during the past four decades. Alexander[6] provided an analysis of axisymmetric concertina mode of failure which forms the basis for many later studies. He formulated the analytical model based on the formation of four plastic hinges by considering that the rigid plastic tube has two straight arms between the hinges. Later, Abramowicz and Jones[7] modified the analysis by introducing curvature in the deforming folds.

It was further refined by Grzebieta[8] by considering that the curvature is confined to only a portion of the fold length. Wierzbicki[9], et al. considered the internal folding in the analysis. In the present work, the variation of internal folding with tube dimensions is studied. Predictions of post-collapse load-compression curve, fold length and average collapse load have been done considering the internal folding as well as the unsymmetrical folding of round tubes.

Composite shells made of layered fibres with epoxy/polyester resin fail in the progressive crushing mode. In the progressive crushing, the layers peal off both inside and outside the shell radius. Thornton[10,11], Farley[12,13] and Hull[14] and their associates have studied the crushing behaviour of composite tubes and the influence of various parameters on the crushing characteristics.

Price and Hull[15] and Mamalis[16], et al. carried out experiments on truncated conical shells under axial compression. They observed progressive crushing failure in the truncated conical shells also under axial compression as was seen in round tubes.

In the present study, the crushing behaviour of round tubes made of glass fabric layer with epoxy resin has been discussed. Analytical expressions were formulated for the prediction of average crush load and crush length in a cycle. The effect of foam on the crushing behaviour was also studied. Experiments on conical shells made of short, randomly oriented glass fibre mat with polyester resin were also carried out and the effect of cone angle on the crushing mode was studied. Analytical expressions have been derived to find the average crush stress and the fold length. The effect of foam on the crushing mode and on the energy absorbing capacity has also been studied.

2. METALLIC SHELLS

Steel and aluminium tubes of diameter (D) 25 mm to 79 mm and thickness(t) 1.2 mm to 2.9 mm were subjected to axial compression. The aluminium tubes were annealed and steel tubes were tested in as received condition to obtain the axisymmetric type of folding. Typical deformation mode of aluminum specimen of $D = 46.9$ mm and $t = 2.9$ mm and a mild steel specimen of $D = 37.4$ mm and $t = 1.6$ mm are shown in Fig. 1.

Typical load-compression curve of such progressive failure of aluminium tube of $D = 49.6$ mm and $t = 1.6$ mm and steel tube of $D = 43$ mm and $t = 1.8$ mm are shown in Figs 2 and 3. From the load-compression curves it is seen that there is intermediate peak for each fold and this peak decreases
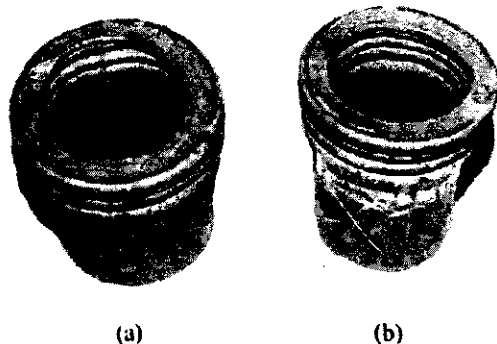

(a)   (b)

Figure 1. Typical deformation of aluminium specimen of (a) $D = 46.9$ mm and $t = 2.9$ mm and (b) a mild steel specimen of $D = 37.4$ mm and $t = 1.6$ mm.

as the folding progresses after the second peak and vanishes after the sixth fold.

Experimental observations reveal that the fold is formed both internally and externally wrt the tube radius. Table 1 gives the internal and external fold lengths. It is seen that the ratio of internal folding to the external folding (N) varies with tube dimensions and is given by the relation:

$$N = \frac{(D/t - A)^{1/n}}{B} \tag{1}$$

where A = 10, B = 225 and n = 3.1.

Table 2 gives the mean collapse load of these specimens calculated from the load-compression curve.

To study the history of deformation of the tubes in concertina mode, several aluminium and

Table 1. Steel tubes of different dimensions and their fold lengths

D_{in} (mm)	t (mm)	L_{in} (mm)	L_{out} (mm)
41.2	1.80	4.80	12.70
25.7	1.20	2.36	6.00
50.9	2.30	5.50	11.90
23.0	2.00	1.90	8.20
28.5	1.85	3.50	9.20
35.8	1.60	4.80	10.30
37.5	1.80	5.40	12.33

Table 2. Experimental and theoretical values of mean collapse load

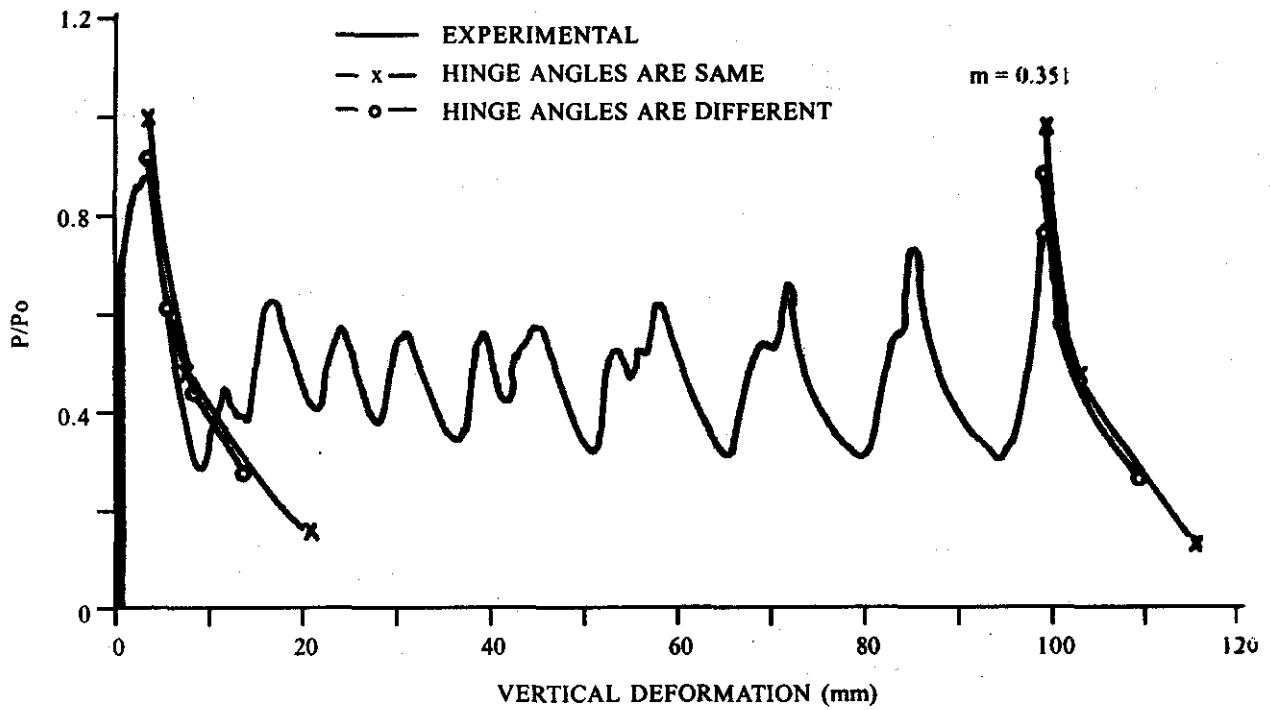| D_{in} (mm)	t (mm)	Expt. values	Theo. values	$\sigma\, MN/m^2$
76.40	2.60	0.482	0.522	152.00
44.00	2.90	0.455	0.410	141.00
48.00	1.60	0.468	0.465	162.00
34.16	1.82	0.450	0.400	120.00
35.50	1.40	0.467	0.450	164.85
34.66	1.73	0.477	0.480	156.00

Figure 2. Typical load-compression curve of aluminium tube of D = 49.6 mm and t = 1.6 mm

steel tubes of identical dimensions were tested for different load levels, namely, first peak, first minimum, second peak, and second minimum. The tested specimens were sectioned vertically at their middle and the deformed profiles were drawn for all the stages using a profile projector. The profile of
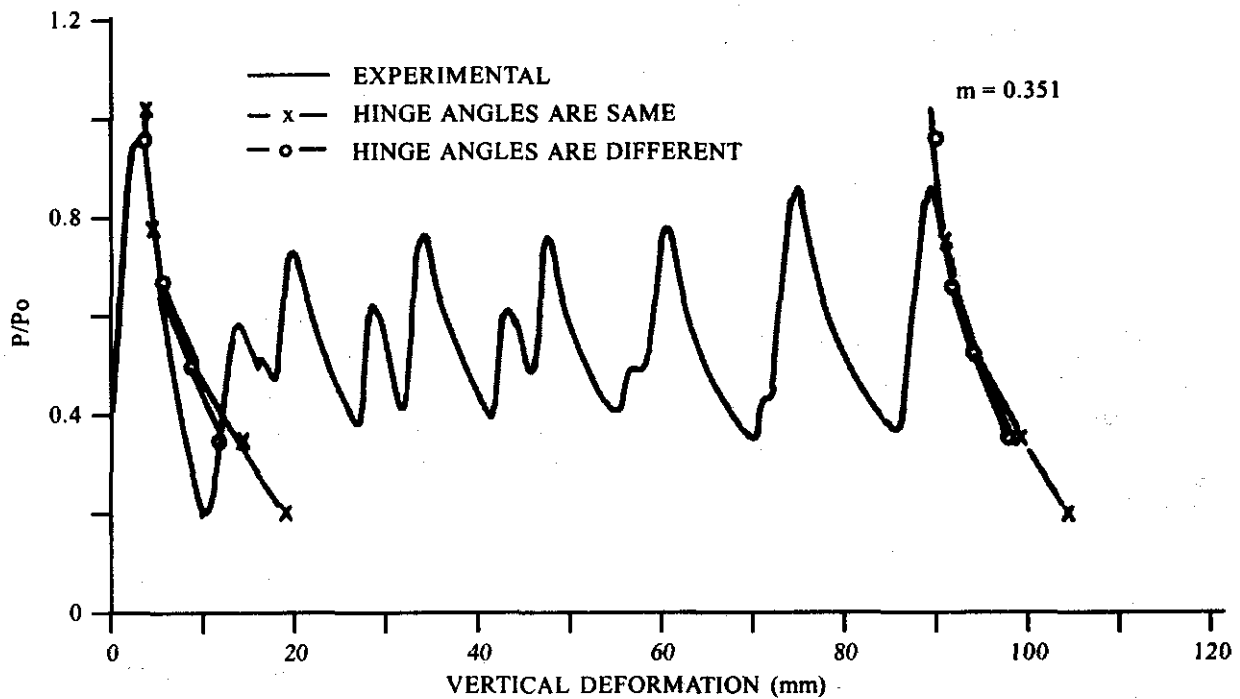

Figure 3. Typical load-compression curve of steel tube of D = 43 mm and t = 1.8 mm

aluminium specimen of $D = 49.6$ mm, $t = 1.6$ mm is shown in Fig. 4. The hinge angle corresponding to the four hinges of a fold was measured and it was shown that the hinge angles, in general, are different.
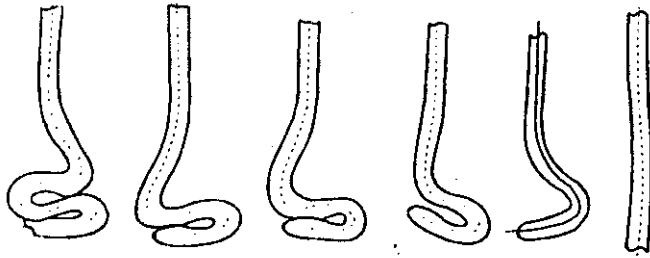

Figure 4. Deformation profile of aluminium specimen of $D = 49.6$ mm, $t = 1.6$ mm.

From the experimental results it is clear that tubes fold internally and externally wrt the mean radius and the amount of internal fold length depends on tube dimensions. Also, the folding pattern is not symmetrical about the middle hinges of a fold and the four hinge angles are different at any particular stage of folding.

Considering the effect of internal folding, an analysis was carried out to find the mean collapse load, fold length, and post-collapse load-compression curve. The analysis is based on the formation of plastic hinges. Typical deformation profile considered for analysis is shown in Fig. 5 in which the internal folding is considered.

Figure 6 shows the profile in which different hinge angles are considered. Analytical expressions are derived for mean collapse load, fold length and load-compression curve for the variation of internal folding. The variation of hoop strain along the length of the tube is complex and only linear variation was considered in the past. However, the expressions are obtained considering the variation of hoop strain along the actual profile. The folding parameter is assumed to vary between 0 to 1/3.

The incremental strain energy is obtained considering the energy involved in bending the
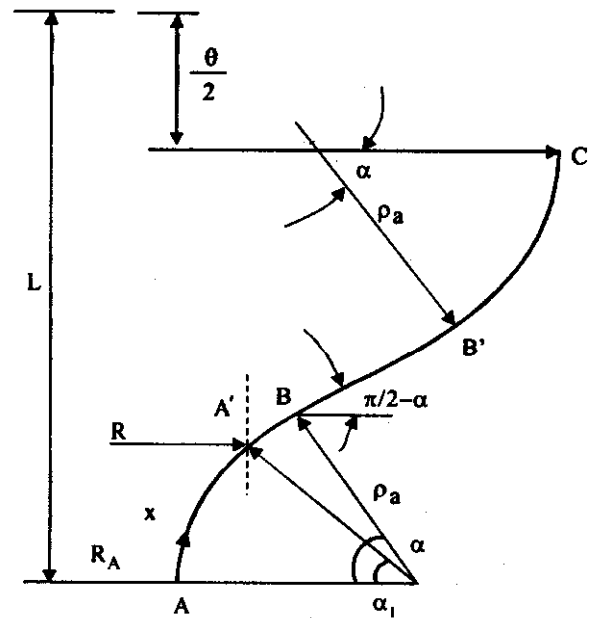

Figure 5. Deformation profile of round tubes (symmetric folding).

four hinges in the axisymmetric fold and the incremental hoop strain between the profile A to C. The expression for fold length is obtained by minimising the total potential energy wrt the half-fold length in a cycle.

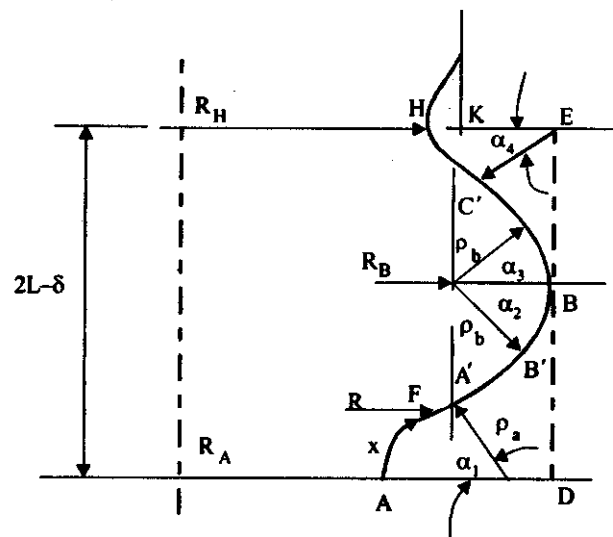The expression for total strain energy is given by

Figure 6. Deformation profile of round tubes (un-symmetric folding).

131

$$W_T = \frac{2}{\sqrt{3}} \pi \sigma_o t^2 \left(1 - \frac{3}{4}\overline{P^2}\right) \left\{2R\alpha_m + LX^*\right\}$$
$$+ 4\pi\sigma_0 tL^2 Y^* \qquad (2)$$

$$X^* = \frac{1}{3}\left\{(1-\cos\alpha_m) + 2\int_0^{\alpha_m} \frac{(\cos\alpha_1 - \cos\alpha)d\alpha}{\alpha}\right\} \qquad (3)$$

$$Y^* = m(m-1)\int_0^{\alpha_m} \frac{\sin\alpha_1}{\alpha} d\alpha + \frac{2}{9}\int_0^{\alpha_m} \frac{\sin\alpha}{\alpha} d\alpha$$
$$+ \frac{1}{9\alpha_m^2}(\sin\alpha_{m1} - \sin\alpha_m)$$
$$+ \frac{1}{3\alpha_m}\left(\frac{1}{3}\cos\alpha_m - m\cos\alpha_{m1}\right) + \frac{1}{6}\sin\alpha_m \qquad (4)$$

Equating this strain energy to the work done by the applied load, one gets:

$$W_p = P\delta_T \qquad (5)$$

where $\delta_T = 2L - t - \frac{2L}{3\alpha}$

and minimising wrt the fold length, the expression for fold length is obtained as

$$L = \frac{1}{4Y^*}\left\{2\overline{P}R\left(1-\frac{1}{3\alpha_m}\right) - \frac{t}{\sqrt{3}}\left(1-\frac{3}{4}\overline{P^2}\right)X^*\right\} \qquad (6)$$

The final expression to find the mean collapse load corresponding to one complete fold is obtained by equating the total internal energy to the total work done by the applied load, and is given by the expression

$$\frac{P_m}{P_o} = \frac{1}{R\left\{2L - t - \frac{2L}{3\alpha}\right\}}$$
$$\left\{\frac{t}{\sqrt{3}}\left(1-\frac{3}{4}\overline{P^2}\right)\left\{2R\alpha_m + LX^*\right\} + 2L^2 Y^*\right\} \qquad (7)$$

The value of α_m is obtained from the expression

$$L - 2L\sin\alpha_m - L\alpha_m\cos\alpha_m + \frac{3\alpha_m t}{2} = 0 \qquad (8)$$

The expression for the post-collapse load-compression curve is obtained by equating the total incremental energy and the total work done by applied load for the incremental displacement. The final expression is obtained as

$$4\pi M_p' \left\{2R + \frac{2L}{3}\left\{\frac{\cos\alpha_1}{\alpha} - \frac{\cos\alpha}{\alpha}\right\} + \frac{L}{3}\sin\alpha\right\}$$
$$+ 4\pi\sigma_0 L^2 t\left(m(2m-1)\frac{\sin\alpha_1}{\alpha} + \frac{2}{9}\frac{\sin\alpha}{\alpha} + \frac{2}{3\alpha^2}\left(m\cos\alpha_1 - \frac{1}{3}\cos\alpha\right)\right.$$
$$\left.+ \frac{2}{9\alpha^3}(\sin\alpha - \sin\alpha_1) + \frac{1}{6}\cos\alpha\right)$$
$$= P\left\{\frac{2L}{3\alpha}\right\}\left\{\frac{2\sin\alpha}{\alpha} - 2\cos\alpha + \alpha\sin\alpha\right\} \qquad (9)$$

The post-collapse load-compression curve thus obtained is compared with the experimental values and is shown in Figs 2 and 3.

3. COMPOSITE SHELLS

The crushing behaviour of composite shells has been widely explored in the application of crashworthiness of vehicles. Empty specimens made from the commercially available glass/epoxy tubes of D/t that varied from 8.5 to 35.0, were subjected to axial compression. The H/D ratio was generally 3. The number of fibre layers in the tubes were confirmed by viewing the small size specimens through an optical microscope and are given in Table 3. Typical crushing mode of the tube is shown in Fig. 7(a) and Fig. 7(b) shows the failure mode of conical shells for different cone angles. A typical load-compression curves are given in Fig. 8.

From Fig. 8 it is seen that in the composite shells after the first peak, the load variation i

132

Table 3. Peak and minimum load values of composite round tubes

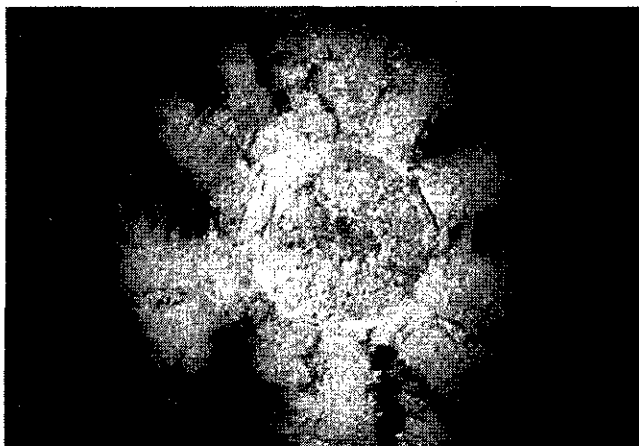| D_o (mm)	t (mm)	No. of layers	P_{ave}	P_{max}/P_{ave}	P_{min}/P_{ave}
17.50	0.85	2	3.00	1.08	0.92
14.40	1.16	3	3.75	1.04	0.95
21.40	1.30	4	5.20	1.15	0.92
22.96	1.90	3	15.00	1.13	0.88
31.90	3.34	5	20.00	1.09	0.91
50.40	2.96	7	23.00	1.13	0.91
54.70	3.50	6	16.00	1.11	0.84
28.56	3.34	7	42.00	1.07	0.93

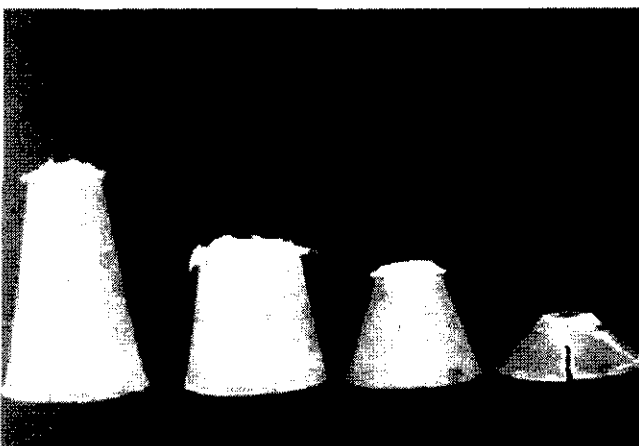
Figure 7(a). Typical crushing mode of a tube

Figure 7(b). Typical failure mode of a conical shell for different cone angles.

oscillatory-type but the amplitude of oscillation is very small compared to round and metallic tubes. The values of peak and minimum are calculated in terms of average load and are given in Table 3. From the deformed tube, it was seen that as crushing progressed, the layers peel off both inside and outside the shell radius. The circumferential outer fibre broke at different locations resulting into petal formation (5 to 8) around the circumference. The layers bending inside were crushed and formed a block as crushing progressed. This block also started sharing the load and there was an increase in the load value in the load-compression curve after 90 per cent of deformation. In thin tubes, the deformation does not stick to the undeformed portion of the tube and there is no petal formation.

Tubes were also filled inside with polyurethane foam and the effect of foam on the energy absorption by the tubes was studied. It was observed that in thick tubes, the presence of foam controls the crack propagation along the length whereas in thin tubes, it encourages the crack to propagate quickly, and hence, there is a reduction in the load carrying capacity of the shell.

Composite conical shells were also fabricated by hand lay up, using short, randomly oriented glass fibre mats with polyester resin and subjected to axial compression. The load-compression curves are shown in Fig. 9. The cone angle was varied from 9.5° to 45.0°. Figure 7(b) shows the failure mode of conical shells for different cone angles. The shells of cone angles between 9.5° and 14.0° had similar type of progressive crushing. Conical shells of semi-cone angle 18.4° start with progressive bending, followed by crushing, and finally formation of a vertical crack, after which the load carrying capacity of the shell comes down immediately. In conical shells of 21°, deformation start with progressive bending, followed by vertical crack formation. In conical shells with cone angle of 45°, the formation of vertical crack started just after the elastic deformation. There was no progressive bending or crushing failure.

Analysis was carried out considering the fracture modes involved in the crushing process. The different
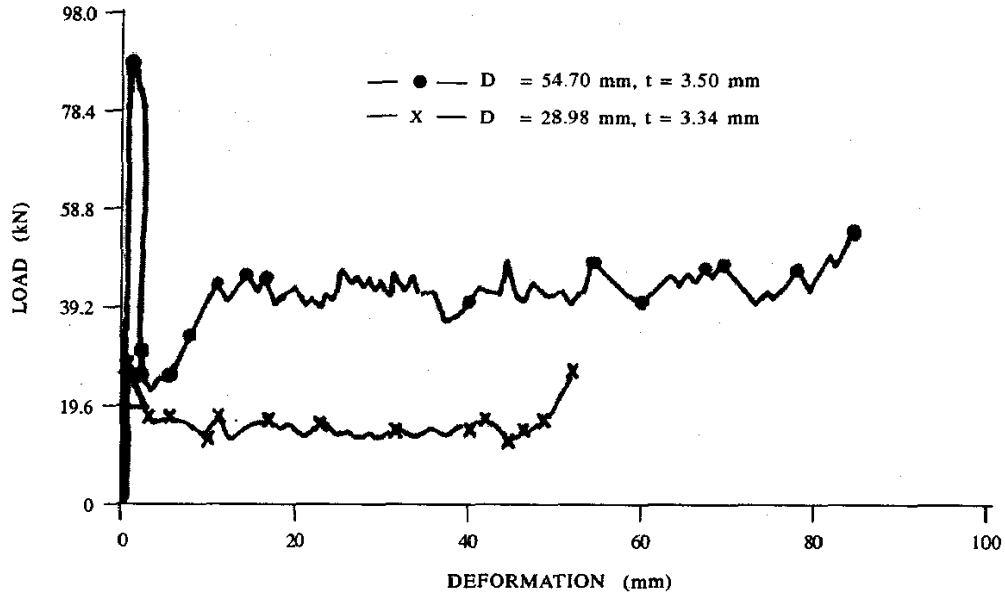
Figure 8. Typical load-compression curves of composite tube crushed more than 90 per cent of its length

fracture modes include: (i) the energy due to central matrix crack in the lengthwise direction, (ii) energy due to bending of layers, both inside and outside the tube radius, (3) energy required to strain the material in the circumferential direction, and the energy required to overcome the friction between the debris and platen.
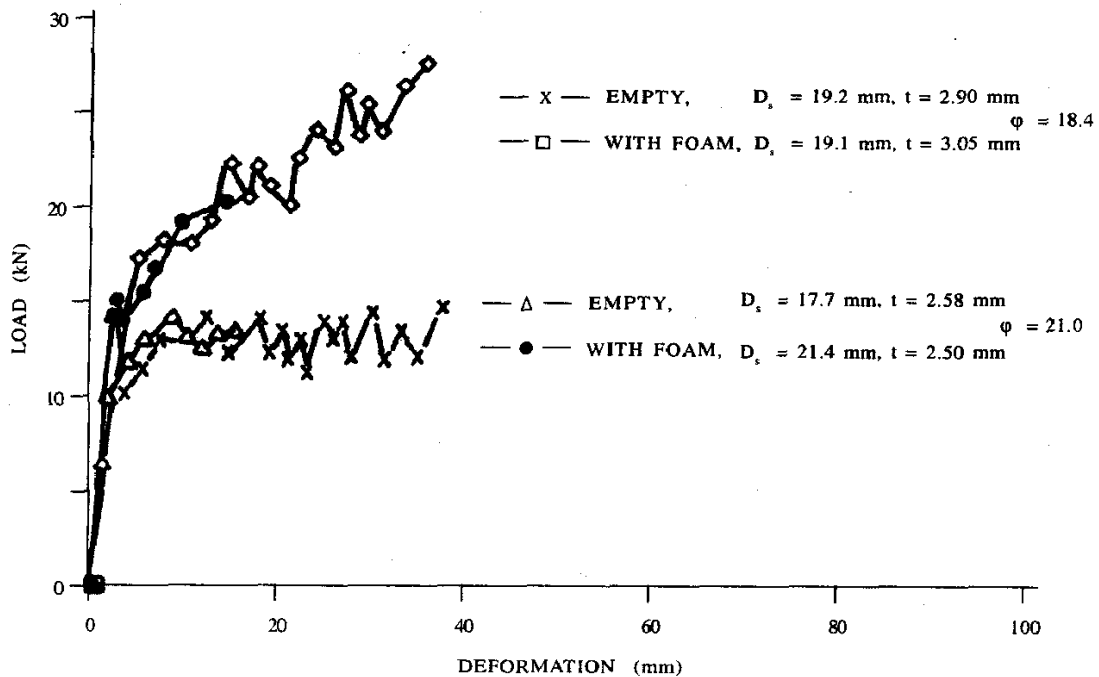

Figure 9. Load-compression curves of empty and foam-filled conical shells

Figures 10 and 11 show the models considered for analysis of conical shells from where the analysis for round tubes has been deduced.

The energy to bend the plies, both inside and outside the shell radius, is given by

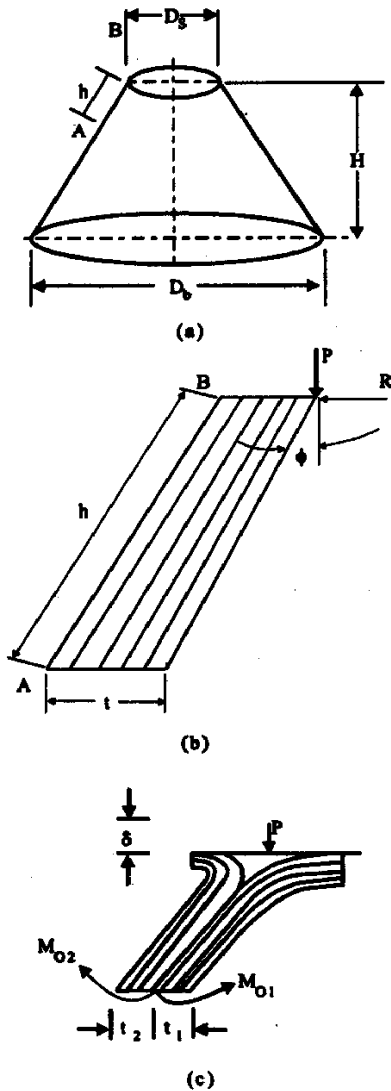$$W_b = \frac{\pi}{2} \sigma_o (t_1^2 \beta + t_2^2 \theta)(R + h \sin \phi) \qquad (10)$$

Figure 10. Conical shell model for analysis: (a) conical shell, (b) undeformed configuration, and (c) deformed configuration.
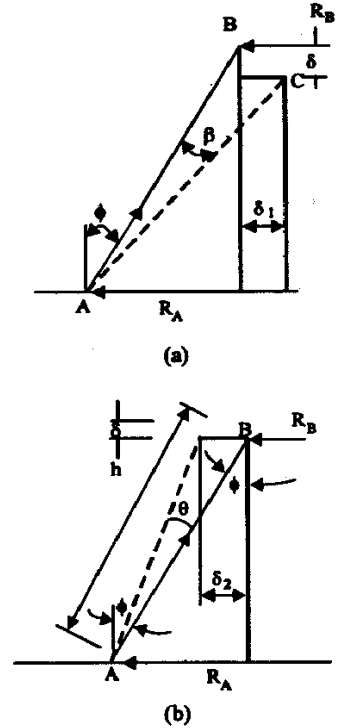
Figure 11. Models considered for analysis of conical shell: (a) layers bending internally and (b) layers bending externally.

The total work due to hoop strain is

$$W_h = \pi \sigma_o h^2 \left[t_1(\sin(\phi + \beta) - \sin \phi) + t_2(\sin \phi - \sin(\phi - \theta)) \right] \qquad (11)$$

The energy required for the propagation of the central crack, which moves along the lengthwise direction is given by

$$W_m = 2\pi\sigma_m(\delta_1 t_1 + \delta_2 t_2)\left(R + \frac{h}{2}\sin \phi\right) \qquad (12)$$

The value of σ_m is given as 26 MPa. The values of δ_1 and δ_2 are given as

$$\delta_1 = h \left[\sin(\phi + \beta) - \sin \phi \right] \qquad (13)$$

$$\delta_2 = h \left[\sin \phi - \sin(\phi - \theta) \right] \qquad (14)$$

The frictional energy is given as

$$W_f = \mu P \delta \tag{15}$$

Equating the total energy to the work done by applied load

$$W_p = P \delta \tag{16}$$

where δ is given as

$$\delta = h[\cos\phi - \cos(\phi + \beta)] \tag{17}$$

The average crush load is obtained as

$$P_m = \frac{\pi}{\delta - \mu\delta_x}\left(0.5\sigma_o(R + h\sin\theta)t^* \right.$$
$$\left. + \left(\sigma_o h^2 + 2\sigma_m\left(R + \frac{h}{2}\sin\phi\right)h\right)t^{**} \right) \tag{18}$$

Minimising the total energy wrt the crush length, the expression for the crush length is obtained as

$$h = \left(\frac{\sigma_o R t^*}{2(\sigma_o + \sigma_m \sin\phi)t^{**}}\right)^{\frac{1}{2}} \tag{19}$$

where

$$t^* = t_1^2\beta + t_2^2\theta$$

$$t^{**} = t_1[\sin(\phi + \beta) - \sin\phi] + t_2[\sin\phi - \sin(\phi - \theta)] \tag{20}$$

In case of cylindrical shells, the expression for average crush load and crush length are given by

$$\sigma_{av} = \frac{1}{\delta - \mu\delta_x}\left[\frac{\sigma_o t\theta}{8} + \sigma_m h\sin\theta + \sigma_o h^2 t\sin\theta\right] \tag{21}$$

$$h = \left(\frac{Rt\theta}{4\sin\theta}\right)^{\frac{1}{2}} \tag{22}$$

The average crush load and the crush length in a cycle for the composite conical shells and round tubes are calculated from the analytical expressions and are compared with the experimental results (Tables 4 and 5). Both the analytical expressions and experimental values match well.

Table 4. Mean crush load and average crush length of composite tubes

R (mm)	t (mm)	σ (kN/m²)		h (mm)	
		Theo. values	Expt. values	Theo. values	Expt. values
8.32	1.00	58.34	59.84	2.08	1.50
10.05	1.30	59.90	60.00	1.81	2.00
14.30	3.34	71.10	69.00	3.46	3.70
24.50	0.90	51.20	34.13	2.37	2.50
27.35	3.50	59.75	61.20	6.25	6.20

Table 5. Mean crush load and average crush length of composite conical shells

D/2 (mm)	t (mm)	φ (deg)	P (kN)		h (mm)	
			Theo. values	Expt. values	Theo. values	Expt. values
12.35	3.15	9.50	24.60	25.50	3.80	5.22
14.99	2.90	14.00	24.80	21.00	4.10	4.63
30.97	2.50	11.00	35.00	42.00	5.50	7.00
34.63	4.00	11.00	68.00	70.00	7.35	10.27

4. CONCLUSION

Round metallic tubes fold both internally and externally wrt the mean radius and the amount of internal folding depends upon tube dimension.

Both the round and the rectangular tubes have similar variation of peak and minimum load value wrt the mean load. In the case of metals, this variation is nearly 30 per cent, but in the case of composite tubes, it is less than 10 per cent. Presence of foam increases the energy absorbing capacity and delays the formation of the vertical crack in conical shells of larger cone angles.

Analytical expressions for the metallic tubes are formulated to find the mean collapse load, fold length, and the post-collapse load-compression curve. Expressions for the mean load and the crush length for the conical shells were formulated and also deduced for cylindrical shells. The analytical results match well with the experimental results in all the cases.

REFERENCES

1. Johnson, W. & Mamalis, A.G. Crashworthiness of vehicles, Mech. Engg. Publications Ltd., London, 1978.

2. Wierzbicki, T. & Jones, N. Structural failure, edited by John Wiley and Sons, 1989.

3. Jones, N. & Wierzbicki, T. Structural crashworthiness and failure, edited by Elsevier Applied Science, 1993.

4. Gupta, N.K. Structural plasticity and impact mechanics, edited by Wiley Eastern, 1992.

5. Abramowicz, W. & Jones, N. Dynamic axial crushing of square tubes. *Int. J. Impact Engg.*, 1984, **2**(2), 179-08.

6. Alexander, J.M. An approximate analysis of the collapse of thin cylindrical shells under axial loading. *Quart. J. Mech. Appl. Math.*, 1960, **13**(1), 10-15.

7. Abramowicz, W. & Jones, N. Dynamic axial crushing of circular tubes. *Int. J. Impact Engg.*, 1984, **2**(3), 263-81.

8. Grzebieta, R.H. An alternative method for determining the behaviour of round stocky tubes subjected to axial crushing load. *Thin-walled Structures*, 1990, **9**, 61-89.

9. Wierzbicki, T.; Bhat, T.S.; Abramowicz W. & Brodkin, D. Alexander revisted- A two folding element model of progressive crushing tubes. *Int. J. Solids Struc.*, 1992, **29**(24), 3269-288.

10. Thornton, P.H. Energy absorption in composite structures. *J. Composite Mater.*, 1979, **13**, 247-63.

11. Thornton, P.H. & Edwards, P.J. Energy absorption in composite tubes. *J. Composite Mater.*, 1982, **16**, 521-45.

12. Farley, G.L. & Jones, R.M. The effect of crushing speed on the energy absorption capability of composite tubes. *J. Composite Mater.*, 1991, **25**, 1314-329.

13. Farley, G.L. & Jones, R.M. Crushing characteristics of continuous fibre-reinforced composite tubes. *J. Composite Mater.*, 1992, **26**(1), 37-50.

14. Hull, D. Axial crushing of fibre-reinforced composite tubes. *In* Structural crashworthiness. Butterworths, London, 1983. pp. 118-35.

15. Price, J.N. & Hull, D. Axial crushing of glass fibre-polyester composite cones. *Composite Sci. Tech.*, 1987, **28**, 211-30.

16. Mamalis, A.G.; Yuan, Y.B. & Viegelahn, G.L. Collapse of thin-walled composite sections subjected to high speed axial loading. *Int. J. Vehicle Design*, 1992, **13**, 564-79.

17. Velmurugan, R. Axial compression of metallic and composite shells. PhD Thesis, Department of Applied Mechanics, IIT Delhi, 1995.